

# Performance of High Mobility MIMO Communications with Doppler Diversity

Xiaoyun Hou, Jie Ling, Dongming Wang

1

**Abstract**—Rapid change of the channels in high-speed mobile communications will lead to difficulties in channel estimation and tracking, but can also provide Doppler diversity. In this paper, the performance of multiple-input multiple-output system with pilot-assisted repetitive coding and spatial multiplexing has been studied. With minimum mean square error (MMSE) channel estimation, an equivalent channel model and the corresponding system model are presented. Based on the random matrix theory, the asymptotic expressions of the normalized achievable sum rate of linear receivers, such as maximal ratio combining (MRC) receiver, MMSE detection and MRC-like receiver are derived. In addition, according to the symbol error rate of the MRC-like receiver, the maximum normalized Doppler diversity order, the minimum coding gain loss can be achieved when the repetition number and the signal to noise ratio tend to infinity and corresponding conditions are also derived. Based on the theoretical results, the impacts of different system configurations and channel parameters on system performance have been demonstrated.

**Index Terms**—Doppler diversity, MIMO, deterministic equivalent, high mobility wireless communication system.

## I. INTRODUCTION

With the popularization of high-speed data services, the demand for high-performance wireless communication on high speed train (HST) is also increasing. However, as a typical application of 4G/5G, the wireless data throughput on HST is still a short board in the cellular communication systems [1], [2]. For high mobility communications, Doppler spread will far exceed the value considered in the design of traditional mid and low speed communication systems. Fast changing small-scale fading and short coherence time will make it difficult to accurately estimate and track channel parameters with pilot signals. The increase of channel estimation error, in turn, can result in degradation of system performance.

Diversity technology is a commonly used anti-fading technology in wireless mobile communications [1]. Since the probability that a statistically independent channel experiences deep fading at the same time is extremely low, the same signal can be transmitted on different channels to achieve diversity gain. In a high mobility scenario, considering the fast change of the channel and transmitting the same signal at different time slots, Doppler diversity can be exploited, thereby the system performance could be improved. In [3] joint multipath-Doppler diversity with perfect channel state

X. Hou and Jie Ling are with Institute of Signal Processing and Transmission, Nanjing University of Posts and Telecommunications, Nanjing, P.R. China (email: houxy@njupt.edu.cn). D. Wang is with the National Mobile Communications Research Lab., Southeast University, Nanjing, 210096, P.R. China (email: wangdm@seu.edu.cn).

information (CSI) was proposed and the validity of Doppler diversity was proved. In high mobility scenarios, the channel estimation error will not be negligible. For a fast fading channel with short coherence time, the channel estimation performance could be worse, while higher Doppler diversity could be exploited [4]. In [5], the performance of Doppler diversity under imperfect channel estimation was studied, and the trade-off between channel estimation error and Doppler diversity was derived. In [6], the results were further extended to single-input multiple-output systems.

Currently, the research on Doppler diversity is mainly focused on single transmit antenna system. Doppler diversity could improve the reliability of the system, while it may lead to low spectral efficiency due to the repetition code. Multiple-input multiple-output (MIMO) technology could make full use of spatial resources and then increase spectral efficiency without additional transmission power. MIMO has become a key technology of many wireless communications standards. By using large-scale antenna arrays at the base station, which is also known as massive MIMO, performance could be further improved [7]–[9]. Massive MIMO has been adopted by the 5G NR standard. In [10] and [11], channel estimation techniques for Massive MIMO systems with high mobility are studied. [12] studied how to overcome Doppler effect with Massive MIMO in high mobility scenarios. The application of Doppler diversity technology in MIMO system could improve the throughput and reliability for high mobility wireless communications. However, under imperfect CSI, the performance of MIMO system using Doppler diversity has not been studied.

In this paper, we study the MIMO system with repetitive coding to achieve Doppler diversity in high mobility communications. Major contributions include:

- 1) For a MIMO system with pilot-assisted repetitive coding and spatial multiplexing, the equivalent channel model of MIMO time-varying channel with imperfect channel estimation was established. The model can be regarded as a more general form of [5], [6].
- 2) For maximum ratio combining (MRC) and MRC-like linear receiver, the asymptotic expression of SINR of the system under Doppler diversity was derived. The deterministic equivalent of the normalization rate for minimum-mean-squared-error (MMSE) receiver was given. The results have shown that the method could obtain a good approximation of the normalization rate even when the antenna size is small and the number of repetitions is small.
- 3) The performance of Doppler diversity including diversity order and minimum coding gain loss for MRC-

like receiver has been derived. The explicit relationship between Doppler diversity gain, coding gain loss and system parameters have been revealed.

The rest of this paper is organized as follows: Section II gives the signal model, channel model, channel estimation and equivalent model of a MIMO system using pilot-assisted repetitive coding. Section III studies the SINR performance of MRC receiver and the SINR performance of MMSE detection under imperfect CSI. Section IV derives the Doppler diversity order and coding gain loss of MRC-like receiver based on the average symbol error rate(SER). Sections V gives numerical results and Section VI summarizes the whole paper.

The symbols used in this paper are described below. Bold lowercase letters and bold uppercase letters represent vectors and matrices, respectively.  $I_M$  denotes the unit matrix of dimension  $M \times M$ .  $|\cdot|$  represents the absolute value of a scalar.  $[\cdot]^T$  and  $[\cdot]^H$  represent vector or matrix transposes and conjugate transposes, respectively.  $\mathbb{C}^{m \times n}$  represents the set of  $m \times n$ -dimensional complex matrices.  $E[\cdot]$  and  $\text{cov}[\cdot]$  represent mathematical expectation and covariance, respectively.  $\text{Tr}[\cdot]$  means the trace of the matrix.  $\text{diag}(\mathbf{x})$  represents a diagonal matrix with  $\mathbf{x}$  as the main diagonal value.  $\mathcal{CN}(0, \sigma^2)$  denotes the distribution of circular symmetric complex Gaussian (CSCG) with mean value 0 and variance  $\sigma^2$ .  $\xrightarrow{a.s.}$  denotes Almost Sure (a.s.) convergence.

## II. PILOT-ASSISTED REPETITIVE PRECODING MIMO SYSTEM MODEL

### A. System Description

Consider an MIMO wireless communications system with  $N_T$  transmitting antennas and  $N_R$  receiving antennas. Assuming the receiver is working with high mobile speed. As shown in Fig.1, a transmission frame includes  $N$  pilot slots and data slots. At the transmitter, the modulated symbols are converted from series to parallel to make multiple data blocks, and then mapped to different transmitting antennas. It is assumed that the data block transmitted on the  $t$ -th transmit antenna is composed of  $K$  independent  $M$ -ary phase-shift-keying (MPSK) symbols, denoted as  $\mathbf{s}_t = [s_{t,1}, \dots, s_{t,K}]^T$ , and the data block is repeatedly transmitted  $N$  times.

In order to obtain CSI, pilot signals are inserted between duplicate data blocks. In order to avoid interference between antennas, different transmitting antennas use orthogonal pilots. For convenience, each transmitting antenna transmits pilot signals at different time. A frame on a transmitting antenna contains pilot and data symbols, expressed as  $\mathbf{x}_t = [\mathbf{p}_t^T, \mathbf{s}_t^T, \dots, \mathbf{p}_t^T, \mathbf{s}_t^T]^T$ . The time interval between adjacent pilot slots is  $T_P = (N_T + K)T$ ,  $T$  is the symbol interval time of the channel. The energy allocated to each pilot symbol and data symbol is  $E_P$  and  $E_C$ , respectively, for a total of  $N_S = (N_T + K)N$  symbols. The energy allocated to each unmodulated data bit can be expressed as

$$E_b = \frac{E_P N + E_C K N}{K \log_2 M}$$

where  $M$  is the modulation order. According to proposition 2 in [13], as long as the pilot interval satisfies  $(N_T + K)T \leq 0.5/f_D$ , accurate channel estimation could be obtained.

Antenna 1	$s_{11}$	$\dots$	$s_{1K}$	$p_1$	0	$s_{11}$	$\dots$	$s_{1K}$	$p_2$	0	$\dots$	$s_{11}$	$\dots$	$s_{1K}$	$p_N$	0
Antenna 2	$s_{21}$	$\dots$	$s_{2K}$	0	$p_1$	$s_{21}$	$\dots$	$s_{2K}$	0	$p_2$	$\dots$	$s_{21}$	$\dots$	$s_{2K}$	0	$p_N$

Fig. 1. Pilot-assisted MIMO system with repetitive coding ( $N_T=2$ )

### B. Channel Model

Let  $h_{t,r}(n)$  denote the discrete-time channel coefficients obtained by the  $n$ -th sampling between the  $t$ -th transmitting antenna and the  $r$ -th receiving antenna. Assuming that the channels between different antenna pairs are independent and undergo Rayleigh fading, that is

$$E[h_{t_1,r_1}(m)h_{t_2,r_2}^*(n)] = 0, \quad r_1 \neq r_2 \text{ or } t_1 \neq t_2 \quad (1)$$

where  $h_{t,r}(n)$  is a symmetric complex Gaussian process with zero mean and satisfies

$$E[h_{t,r}(m)h_{t,r}^*(n)] = J_0(2\pi f_D |m - n|T) \quad (2)$$

In (2),  $J_0(\cdot)$  is the first kind of zero-order Bessel function,  $f_D$  is the maximum Doppler spread. In this paper, it is assumed that  $f_D$  is known and the estimation of  $f_D$  can be referred to [14].

### C. Pilot Signal Model

Denote the timing indices of the  $n$ -th pilot symbol on the  $t$ -th transmitting antenna in a transmission frame as:

$$i_{t,n} = t + (n - 1)(N_T + K), \quad n=1, \dots, N.$$

The pilot symbols received by the  $r$ -th receiving antenna from the  $t$ -th transmitting antenna can be expressed as:

$$\mathbf{y}_{P,t,r} = \sqrt{E_P} \mathbf{X}_P \mathbf{h}_{P,t,r} + \mathbf{z}_{P,t,r}, \quad (3)$$

where

$$\begin{aligned} \mathbf{y}_{P,t,r} &= [y_{r,i_{t,1}} \quad \dots \quad y_{r,i_{t,N}}]^T \in \mathbb{C}^{N \times 1}, \\ \mathbf{X}_P &= \text{diag}([p_1 \quad \dots \quad p_N]), \\ \mathbf{h}_{P,t,r} &= [h_{t,r}(i_{t,1}) \quad \dots \quad h_{t,r}(i_{t,N})]^T \in \mathbb{C}^{N \times 1}, \\ \mathbf{z}_{P,t,r} &= [z_{r,i_{t,1}} \quad \dots \quad z_{r,i_{t,N}}]^T \in \mathbb{C}^{N \times 1} \end{aligned}$$

are received pilot signal vector, transmitted pilot matrix, channel vector and additive white Gaussian noise(AWGN) vector. It is assumed that the noise vector is a zero-mean CSCG random vector with covariance matrix  $\sigma^2 \mathbf{I}_N$ .

### D. MMSE Channel Estimation

The timing indices of the  $k$ -th data symbol on the  $t$ -th transmitting antenna in a transmission frame can be expressed as:

$$k_n = N_T + k + (n - 1)(N_T + K), \quad n=1, \dots, N.$$

Then the vector of all channel coefficients corresponding to the  $k$ -th data symbol between the  $t$ -th transmitting antenna and the  $r$ -th receiving antenna is

$$\mathbf{h}_{t,r,k} = [h_{t,r}(k_1) \quad \dots \quad h_{t,r}(k_N)]^T.$$

With the received  $N$  slots pilot signals and the known channel statistics, and according to the principle of MMSE, the channel estimation of  $\hat{\mathbf{h}}_{t,r,k}$  can be expressed as [5],

$$\hat{\mathbf{h}}_{t,r,k} = \sqrt{E_p} \mathbf{R}_{P,t,k} \mathbf{X}_P^H (E_P \mathbf{X}_P \mathbf{R}_P \mathbf{X}_P^H + \sigma^2 \mathbf{I}_N)^{-1} \mathbf{y}_{P,t,r}, \quad (4)$$

where

$$\mathbf{R}_P = \mathbb{E} [\mathbf{h}_{P,t,r} \mathbf{h}_{P,t,r}^H] \in \mathcal{R}^{N \times N},$$

is a Toeplitz matrix, and its first column is given by

$$\mathbf{r}_P = [\rho_0 \ \cdots \ \rho_{N-1}]^T, \rho_n = J_0(2\pi f_D |n| T_p).$$

$\mathbf{R}_P$  is not related to  $t$  and  $r$ . Because of the symmetry, the first column is the same as the first row. In (4),

$$\mathbf{R}_{P,t,k} = \mathbb{E} [\mathbf{h}_{t,r,k} \mathbf{h}_{P,t,r}^H] \in \mathcal{R}^{N \times N},$$

is also a Toeplitz matrix. Because the first kind of zero-order Bessel function  $J_0(x)$  is even when  $x$  is real, the first column and the first row can be written as

$$[\tau_{t,0} \ \tau_{t,-1} \ \cdots \ \tau_{t,-N+1}]^T, [\tau_{t,0} \ \tau_{t,1} \ \cdots \ \tau_{t,N-1}]$$

where

$$\tau_{t,n} = J_0(2\pi T [N_T + k - t - n(N_T + K)]),$$

is not related to  $r$ . When orthogonal pilot sequences are used, that is,  $\mathbf{X}_P \mathbf{X}_P^H = \mathbf{I}_N$ , by using the following matrix inversion equation,

$$\mathbf{CD}(\mathbf{A} + \mathbf{BCD}) = (\mathbf{C}^{-1} + \mathbf{DC}^{-1}\mathbf{B})^{-1} \mathbf{DA}^{-1},$$

(4) can be rewritten as

$$\hat{\mathbf{h}}_{t,r,k} = \sqrt{E_p} \mathbf{R}_{P,t,k} (E_P \mathbf{R}_P + \sigma^2 \mathbf{I}_N)^{-1} \mathbf{X}_P^H \mathbf{y}_{P,t,r}. \quad (5)$$

Define the channel estimation error as,

$$\tilde{\mathbf{h}}_{t,r,k} = \mathbf{h}_{t,r,k} - \hat{\mathbf{h}}_{t,r,k}.$$

Then, according to the MMSE estimation principle, the covariance matrices for the estimated channel vector  $\hat{\mathbf{h}}_{t,r,k}$  and the error  $\tilde{\mathbf{h}}_{t,r,k}$  can be expressed as [15],

$$\hat{\mathbf{R}}_{t,k} = \mathbf{R}_{P,t,k} \left( \mathbf{R}_P + \frac{1}{\gamma_p} \mathbf{I}_N \right)^{-1} \mathbf{R}_{P,t,k}^H, \quad (6)$$

$$\tilde{\mathbf{R}}_{t,k} = \mathbf{R}_k - \mathbf{R}_{P,t,k} \left( \mathbf{R}_P + \frac{1}{\gamma_p} \mathbf{I}_N \right)^{-1} \mathbf{R}_{P,t,k}^H, \quad (7)$$

respectively, where  $\gamma_p = E_p/\sigma^2$  is the pilot signal to noise ratio and  $\mathbf{R}_k = \mathbb{E} [\mathbf{h}_{t,r,k} \mathbf{h}_{t,r,k}^H]$ . According to the frame structure and the properties of Bessel function,  $\mathbf{R}_k = \mathbf{R}_P$ .

#### E. Equivalent System Model

Let

$$\mathbf{y}_k = [\mathbf{y}_{1,k}^T, \cdots, \mathbf{y}_{N_R,k}^T]^T,$$

denote the collection of the  $N$  slots received signals of all receiving antennas corresponding to the  $k$ -th data vector  $\mathbf{s}_k$ .  $\mathbf{y}_k$  can be expressed as,

$$\mathbf{y}_k = \sqrt{E_C} \mathbf{H}_k \mathbf{s}_k + \mathbf{z}_k, \quad (8)$$

where the channel matrix  $\mathbf{H}_k$  is denoted as:

$$\mathbf{H}_k = [\mathbf{H}_{1,k}^T \ \cdots \ \mathbf{H}_{N_R,k}^T]^T$$

$$\mathbf{H}_{r,k} = [\mathbf{h}_{1,r,k} \ \cdots \ \mathbf{h}_{t,r,k} \ \cdots \ \mathbf{h}_{N_T,r,k}]$$

According to the definition of channel estimation error, the channel matrix can be expressed as,

$$\mathbf{H}_k = \hat{\mathbf{H}}_k + \tilde{\mathbf{H}}_k. \quad (9)$$

Then, (8) can be rewritten as

$$\mathbf{y}_k = \sqrt{E_C} \hat{\mathbf{H}}_k \mathbf{s}_k + \hat{\mathbf{z}}_k, \quad (10)$$

where

$$\hat{\mathbf{z}}_k = \sqrt{E_C} \tilde{\mathbf{H}}_k \mathbf{s}_k + \mathbf{z}_k.$$

With (7), we have

$$\text{cov}(\hat{\mathbf{z}}_k, \hat{\mathbf{z}}_k) = E_C \tilde{\mathbf{R}}_k = \mathbf{I}_{N_R} \otimes \left( E_C \sum_{t=1}^{N_T} \tilde{\mathbf{R}}_{t,k} + \sigma^2 \mathbf{I}_N \right). \quad (11)$$

Moreover, the covariance matrix of the  $t$ -th column of  $\hat{\mathbf{H}}_k$  can be expressed as,

$$\text{cov}(\hat{\mathbf{h}}_{t,k}, \hat{\mathbf{h}}_{t,k}) = \mathbf{I}_{N_R} \otimes \hat{\mathbf{R}}_{t,k}. \quad (12)$$

Remark: We establish a pilot-assisted repetitive precoding MIMO system signal model under imperfect CSI. It can be seen that for the  $k$ -th transmission vector  $\mathbf{s}_k$  in the data block, the covariance matrices of different columns of its corresponding channel matrix  $\hat{\mathbf{H}}_k$  are different. This is mainly due to the use of time division to transmit pilots of different antennas. This also brings difficulties for further analysis of system performance.

### III. CAPACITY ANALYSIS OF MRC, MMSE AND MRC-LIKE RECEIVER

Next, we will study the spectral efficiency of the system represented in formula (10) with different receivers. We first study the MRC receiver and give its asymptotic rate analysis. Then the deterministic equivalent for the SINR of MMSE receiver is studied. Finally, the asymptotic rate of MRC-like receivers is analyzed.

#### A. Asymptotic Achievable Sum-Rate of MRC Detection

When the receiver uses MRC receiver, the detection of the  $k$ -th data symbol of the  $t$ -th transmitting antenna can be expressed as

$$\hat{s}_{\text{MRC},t,k} = E_C \hat{\mathbf{h}}_{t,k}^H \hat{\mathbf{h}}_{t,k} s_{t,k} + E_C \sum_{l=1, l \neq t}^{N_T} \hat{\mathbf{h}}_{t,k}^H \hat{\mathbf{h}}_{l,k} s_{l,k} + \sqrt{E_C} \hat{\mathbf{h}}_{t,k}^H \hat{\mathbf{z}}_k. \quad (13)$$

So the corresponding SINR can be expressed as [16],

$$\gamma_{\text{MRC},t,k} = \frac{|\hat{\mathbf{h}}_{t,k}^H \hat{\mathbf{h}}_{t,k}|^2}{\hat{\mathbf{h}}_{t,k}^H (\hat{\mathbf{H}}_{[t],k} \hat{\mathbf{H}}_{[t],k}^H + \tilde{\mathbf{R}}_k) \hat{\mathbf{h}}_{t,k}} \quad (14)$$

where  $\hat{\mathbf{H}}_{[t],k}$  is the result of  $\hat{\mathbf{H}}_k$  removing the  $t$ -th column. According to Theorem 3.4 of [17], when  $NN_R \rightarrow \infty$ :

$$\begin{aligned} \frac{1}{NN_R} \hat{\mathbf{h}}_{t,k}^H \hat{\mathbf{h}}_{t,k} &\xrightarrow{a.s.} \frac{1}{N} \text{Tr} \left( \hat{\mathbf{R}}_{t,k} \right) \quad (15) \\ \frac{1}{NN_R} \hat{\mathbf{h}}_{t,k}^H \left( \hat{\mathbf{H}}_{[t],k} \hat{\mathbf{H}}_{[t],k}^H + \tilde{\mathbf{R}}_k \right) \hat{\mathbf{h}}_{t,k} &\xrightarrow{a.s.} \\ \frac{1}{NN_R} \text{Tr} \left( \left( \mathbf{I}_{N_R} \otimes \hat{\mathbf{R}}_{t,k} \right) \left( \hat{\mathbf{H}}_{[t],k} \hat{\mathbf{H}}_{[t],k}^H + \tilde{\mathbf{R}}_k \right) \right) &\xrightarrow{a.s.} \\ \frac{1}{N} \text{Tr} \left( \sum_{l_1=1, l_1 \neq t}^{N_T} \hat{\mathbf{R}}_{t,k} \hat{\mathbf{R}}_{l_1,k} + \hat{\mathbf{R}}_{t,k} \left( \sum_{l_2=1}^{N_T} \tilde{\mathbf{R}}_{l_2,k} + \frac{1}{\gamma_C} \mathbf{I}_N \right) \right) \end{aligned} \quad (16)$$

where  $\gamma_C = E_C/\sigma^2$  is the data signal to noise ratio. By further using Theorem 3.4 and 3.7 of [17] to (16) and together with (15), we can get:

$$\gamma_{\text{MRC},t,k} \xrightarrow{a.s.} \bar{\gamma}_{\text{MRC},t,k} \quad (17)$$

where  $\bar{\gamma}_{\text{MRC},t,k}$  is given at the bottom of this page. Since repetitive coding requires multiple time slots to transmit the same data block, we define the normalized achievable sum-rate as follows to better reflect the spectral efficiency of the system:

$$R_{\text{MRC},k} = \frac{1}{N} \sum_{t=1}^{N_T} \log_2 (1 + \gamma_{\text{MRC},t,k}) \quad (19)$$

From the Remark 5 of [18], by the control convergence theorem, it satisfies:

$$R_{\text{MRC},k} - \frac{1}{N} \sum_{t=1}^{N_T} \log_2 (1 + \bar{\gamma}_{\text{MRC},t,k}) \xrightarrow{a.s.} 0 \quad (20)$$

According to (20) asymptotic results, we can get an approximate expression of normalized sum-rate of MRC.

### B. Asymptotic Achievable Sum-Rate of MMSE Detection

In this section, we analyze the SINR of MMSE receiver under imperfect CSI, and present a method to calculate the normalized achievable sum-rate of the system based on deterministic equivalent.

When linear MMSE detection is used, the output SINR of the  $k$ -th symbol on the  $t$ -th transmitting antenna can be expressed as

$$\gamma_{\text{MMSE},t,k} = \hat{\mathbf{h}}_{t,k}^H \left( \hat{\mathbf{H}}_{[t],k} \hat{\mathbf{H}}_{[t],k}^H + \tilde{\mathbf{R}}_k \right)^{-1} \hat{\mathbf{h}}_{t,k} \quad (21)$$

Let

$$\check{\mathbf{h}}_{t,k} = \left[ \mathbf{I}_{N_R} \otimes \left( \sum_{l=1}^{N_T} \tilde{\mathbf{R}}_{l,k} + \frac{1}{\gamma_C} \mathbf{I}_N \right)^{-\frac{1}{2}} \right] \hat{\mathbf{h}}_{t,k}.$$

$$\check{\mathbf{H}}_k = \left[ \begin{array}{cccc} \check{\mathbf{h}}_{1,k} & \cdots & \check{\mathbf{h}}_{N_T,k} \end{array} \right].$$

Then we have

$$\gamma_{\text{MMSE},t,k} = \check{\mathbf{h}}_{t,k}^H \left( \check{\mathbf{H}}_{[t],k} \check{\mathbf{H}}_{[t],k}^H + \mathbf{I}_{NN_R} \right)^{-1} \check{\mathbf{h}}_{t,k}$$

$\check{\mathbf{H}}_{[t],k}$  is a sub-matrix of  $\check{\mathbf{H}}_k$  with removing column  $t$ . Since

$$\begin{aligned} \text{cov} \left( \check{\mathbf{h}}_{t,k}, \check{\mathbf{h}}_{t,k} \right) &= \mathbf{I}_{N_R} \otimes \\ &\left( \left( \sum_{l=1}^{N_T} \tilde{\mathbf{R}}_{l,k} + \frac{1}{\gamma_C} \mathbf{I}_N \right)^{-\frac{1}{2}} \hat{\mathbf{R}}_{t,k} \left( \sum_{l=1}^{N_T} \tilde{\mathbf{R}}_{l,k} + \frac{1}{\gamma_C} \mathbf{I}_N \right)^{-\frac{1}{2}} \right). \end{aligned}$$

According to Theorem 3.4 of [17] when  $NN_R \rightarrow \infty$ :

$$\frac{1}{NN_R} \gamma_{\text{MMSE},t,k} \xrightarrow{a.s.} m_{\mathbf{B},\mathbf{Q}}. \quad (22)$$

Define

$$\mathbf{B} \triangleq \check{\mathbf{H}}_{[t],k} \check{\mathbf{H}}_{[t],k}^H$$

$$\mathbf{Q} \triangleq \text{cov} \left( \check{\mathbf{h}}_{t,k}, \check{\mathbf{h}}_{t,k} \right)$$

$$m_{\mathbf{B},\mathbf{Q}} \triangleq \frac{1}{NN_R} \text{Tr} \left[ \mathbf{Q} (\mathbf{B} + \mathbf{I}_{NN_R})^{-1} \right]$$

According to Theorem 1 of [18]:

$$m_{\mathbf{B},\mathbf{Q}} \xrightarrow{a.s.} m_{\mathbf{B},\mathbf{Q}}^0 \quad (23)$$

In (23),

$$m_{\mathbf{B},\mathbf{Q}}^0 = \frac{1}{NN_R} \text{Tr} (\mathbf{Q} \mathbf{T}) \quad (24)$$

$$\mathbf{T} = \left( \sum_{l=1, l \neq t}^{N_T} \frac{\Phi_l}{1 + e_l} + \mathbf{I}_{NN_R} \right)^{-1} \quad (25)$$

$$\Phi_l = \text{cov} \left( \check{\mathbf{h}}_{l,k}, \check{\mathbf{h}}_{l,k} \right) \quad (26)$$

where  $e_l$  is the only solution to the following equation:

$$e_l = \text{Tr} (\Phi_l \mathbf{T}) \quad (27)$$

Matrix  $\mathbf{T}$  can be obtained by iterative calculations using (25)(26)(27). Then deterministic equivalent of  $\gamma_{\text{MMSE},t,k}$  can be obtained without knowing the exact value of  $\hat{\mathbf{h}}_{t,k}$ . Similarly, from the Remark 5 of [18], by the control convergence theorem, we can get the asymptotic value of the normalized achievable sum-rate of MMSE receiver.

$$\bar{\gamma}_{\text{MRC},t,k} = \frac{N_R \text{Tr}^2 (\hat{\mathbf{R}}_{t,k})}{\sum_{l_1=1, l_1 \neq t}^{N_T} \text{Tr} (\hat{\mathbf{R}}_{l_1,k} \hat{\mathbf{R}}_{t,k}) + \text{Tr} \left( \hat{\mathbf{R}}_{t,k} \left( \sum_{l_2=1}^{N_T} \tilde{\mathbf{R}}_{l_2,k} + \frac{1}{\gamma_C} \mathbf{I}_N \right) \right)} \quad (18)$$

### C. Asymptotic Achievable Sum-Rate of MRC-like Receiver

To further improve the performance of MRC receiver, we also consider a MRC-like receiver. To detect the  $k$ -th data symbol of the  $t$ -th transmitting antenna, we first perform the whitening of interference-plus-noise with the statistics of the CSI and then do the MRC receiver. Rewrite (10) as

$$\mathbf{y}_k = \sqrt{E_C} \hat{\mathbf{h}}_{t,k} s_{t,k} + \check{\mathbf{z}}_k, \quad (28)$$

where

$$\check{\mathbf{z}}_k = \sqrt{E_C} \sum_{l=1, l \neq t}^{N_T} \hat{\mathbf{h}}_{l,k} s_{l,k} + \hat{\mathbf{z}}_k.$$

The operation for the whitening of interference-plus-noise is denoted as

$$\bar{\mathbf{y}}_k = \mathbf{R}_{W,t,k} \mathbf{y}_k, \quad (29)$$

where

$$\mathbf{R}_{W,t,k} \triangleq \left[ \mathbf{I}_{N_R} \otimes \left( E_C \sum_{l_1=1, l_1 \neq t}^{N_T} \hat{\mathbf{R}}_{l_1,k} \right. \right. \\ \left. \left. + E_C \sum_{l_2=1}^{N_T} \tilde{\mathbf{R}}_{l_2,k} + \sigma^2 \mathbf{I}_N \right) \right]^{-\frac{1}{2}}.$$

The signal model is now rewritten as:

$$\bar{\mathbf{y}}_k = \sqrt{E_C} \bar{\mathbf{H}}_k \bar{s}_k + \bar{\mathbf{z}}_k, \quad (30)$$

where  $\bar{\mathbf{H}}_k = \mathbf{R}_{W,t,k} \hat{\mathbf{H}}_k$ . Then, the estimated data symbols are given by

$$\hat{s}_{M\text{-MRC},t,k} = \sqrt{E_C} \bar{\mathbf{h}}_{t,k}^H \bar{\mathbf{y}}_k \quad (31)$$

The SINR of MRC-like can be expressed as (32), which is shown on the bottom of this page. Similar to MRC receiver, by using Theorem 3.4 and 3.7 of [17], we have

$$\gamma_{M\text{-MRC},t,k} \xrightarrow{a.s.} \bar{\gamma}_{M\text{-MRC},t,k}, \quad (33)$$

where

$$\bar{\gamma}_{M\text{-MRC},t,k} \xrightarrow{a.s.} N_R \text{Tr} \left( \left( \hat{\mathbf{R}}_{t,k} \right)^{\frac{1}{2}} \right. \\ \left. \times \left( \sum_{l_1=1, l_1 \neq t}^{N_T} \hat{\mathbf{R}}_{l_1,k} + \sum_{l_2=1}^{N_T} \tilde{\mathbf{R}}_{l_2,k} + \frac{1}{\gamma_C} \mathbf{I}_N \right)^{-1} \left( \hat{\mathbf{R}}_{t,k} \right)^{\frac{1}{2}} \right) \quad (34)$$

Define

$$R_{M\text{-MRC},k} = \frac{1}{N} \sum_{t=1}^{N_T} \log_2 (1 + \gamma_{M\text{-MRC},t,k}). \quad (35)$$

Also by the control convergence theorem,

$$R_{M\text{-MRC},k} - \frac{1}{N} \sum_{t=1}^{N_T} \log_2 (1 + \bar{\gamma}_{M\text{-MRC},t,k}) \xrightarrow{a.s.} 0 \quad (36)$$

We will show in the simulations that when  $N$  is large, the performance of the MRC-like receiver will approach MMSE.

### IV. DOPPLER DIVERSITY ORDER AND CODING GAIN LOSS FOR MRC-LIKE RECEIVERS

In this section, we first obtain the average SER expression when the system uses MRC-like receivers. Based on the SER expression, we study the maximum Doppler diversity order and the minimum coding gain loss that can be achieved in this case.

#### A. Average SER of MRC-like Detection

For the convenience of analysis, we assume that the specific CSI corresponding to other transmitting antennas is unknown when estimating the data symbols of the  $t$ -th antenna, and  $\hat{s}_{M\text{-MRC},t,k}$  obeys the Gaussian distribution with  $s_{t,k}$  and  $\bar{\mathbf{h}}_{t,k}$  as conditions. The conditional mean and conditional variance can be given by,

$$u_{\hat{s}|\bar{\mathbf{h}},s,t,k} = E_C \bar{\mathbf{h}}_{t,k}^H \bar{\mathbf{h}}_{t,k} s_{t,k},$$

$$\sigma_{\hat{s}|\bar{\mathbf{h}},s,t,k}^2 = E_C \bar{\mathbf{h}}_{t,k}^H \bar{\mathbf{h}}_{t,k}.$$

According to Appendix C in [5], the conditional probability density function of  $\hat{s}_{M\text{-MRC},t,k}$  is integrated according to the range of decision domain. By using the symmetry of MPSK constellation points and the moment generating function of complex Gaussian random vector quadratic form, the average bit error rate of MRC-like detection can be obtained,

$$\bar{P}_{e,t,k} = \frac{1}{\pi} \int_0^{\Theta} \left[ \det \left( \mathbf{I}_N + \frac{C_M}{\sin^2 \theta} \mathbf{A}_{t,k} \right) \right]^{-N_R} d\theta \quad (37)$$

where  $\Theta = \pi - \pi/M$ ,  $C_M = \sin^2(\pi/M)$ ,

$$\mathbf{A}_{t,k} = \hat{\mathbf{R}}_{t,k} \left( \sum_{l=1, l \neq t}^{N_T} \hat{\mathbf{R}}_{l,k} + \left( \sum_{t=1}^{N_T} \tilde{\mathbf{R}}_{t,k} + \frac{1}{\gamma_C} \mathbf{I}_N \right) \right)^{-1} \quad (38)$$

#### B. Doppler Diversity Order of MRC-like Detection

Based on the Jensen's inequality and the fact  $\sin^2 \theta \leq 1$ , the upper and lower bounds of  $\log(\bar{P}_{e,t,k})$  can be obtained.

$$\eta_U = \log v - N_R \log [\det(\mathbf{I}_N + C_M \mathbf{A}_{t,k})] \quad (39)$$

$$\eta_L = \log v - \frac{N_R}{\pi v} \int_0^{\pi v} \log [\det(\mathbf{I}_N + \frac{C_M}{\sin^2 \theta} \mathbf{A}_{t,k})] d\theta \quad (40)$$

Among them  $v = 1 - 1/M$ . From Lemma 2 of [19], when  $NN_R \rightarrow \infty$ :

$$\mathbf{A}_{t,k} \xrightarrow{a.s.} \mathbf{U}_N^H \mathbf{D} \mathbf{U}_N \quad (41)$$

$$\gamma_{M\text{-MRC},t,k} = \frac{\left| \bar{\mathbf{h}}_{t,k}^H \bar{\mathbf{h}}_{t,k} \right|^2}{\bar{\mathbf{h}}_{t,k}^H \left( \bar{\mathbf{H}}_{[t],k} \bar{\mathbf{H}}_{[t],k}^H + \mathbf{R}_{W,t,k} \tilde{\mathbf{R}}_k \mathbf{R}_{W,t,k}^H \right) \bar{\mathbf{h}}_{t,k}} \quad (32)$$

$U_N$  is  $N$ -dimensional unitary discrete Fourier transform matrix,  $\mathbf{D}$  is a diagonal matrix with

$$(\mathbf{D})_{n,n} = \begin{pmatrix} N_T - 1 \\ + \left( \frac{\Lambda_{PP}^2 (2\pi \frac{n-1}{N})}{\frac{N_T}{\gamma_P} \Lambda_{PP} (2\pi \frac{n-1}{N}) + \frac{1}{\gamma_C} \Lambda_{PP} (2\pi \frac{n-1}{N}) + \frac{1}{\gamma_P \gamma_C}} \right)^{-1} \right)^{-1}$$

$$\Lambda_{PP}(\Omega) = \frac{2\text{rect}(\frac{\Omega}{2\omega_D T_P})}{\sqrt{(\omega_D T_P)^2 - \Omega^2}}, \quad -\pi \leq \Omega \leq \pi$$

where  $\omega_D = 2\pi f_D$ . It can be found that  $\mathbf{D}$  is not related to  $t$  and  $k$ , and the average SER at this time is  $\bar{P}_e$ . Define the energy required to transmit a coded data symbol as

$$E_0 = (1/K) E_P + E_C,$$

and the corresponding SNR  $\gamma_0 = E_0 / \sigma^2$ . Define

$$\Psi_{t,k}(\gamma_0) = \det(\mathbf{I}_N + c\mathbf{A}_{t,k}),$$

where  $c$  is a constant. Let

$$\delta = \omega_D T_P, \quad \gamma_t = N_T \gamma_C + \gamma_P, \quad \gamma_P = b \gamma_C^\xi$$

where  $b$  and  $\xi$  are constants. According to the Appendix D of [5], it can be inferred that:

$$\begin{aligned} & \lim_{N \rightarrow \infty} \frac{\log(\Psi_{t,k}(\gamma_0))}{N} \\ &= \frac{\delta}{\pi} \log(4\gamma_P \gamma_C c) - \frac{\delta \log(2\delta) - 2\delta}{\pi} \\ & \quad - \frac{\delta \log(2\gamma_t)}{\pi} - \left( \gamma_t - \frac{\sqrt{4\gamma_t^2 - \delta^2}}{2} \right) \\ & \quad - \frac{\sqrt{4\gamma_t^2 - \delta^2}}{\pi} \arctan \left( \sqrt{\frac{\delta^2}{4\gamma_t^2 - \delta^2}} \right) \end{aligned} \quad (42)$$

Consider the definition of normalized Doppler diversity order:

$$D = - \lim_{\substack{\gamma_0 \rightarrow \infty \\ N \rightarrow \infty}} \frac{\log(\bar{P}_e)}{N T_P \log(\gamma_0)} \quad (43)$$

(39) and (40) are substituted into (43) to calculate the upper and lower bounds of the order of Doppler diversity  $D_U$  and  $D_L$ . By combining result with formulas (41) and (42),  $c$  is  $C_M$  in the upper bound and  $C_M / \sin^2 \theta$  in the lower bound,

$$D_U = D_L = - \lim_{\substack{\gamma_0 \rightarrow \infty \\ N \rightarrow \infty}} \frac{N_R \log(\Psi_{t,k}(\gamma_0))}{N T_P \log(\gamma_0)} = \begin{cases} 2f_D N_R \xi, & \xi \leq 1 \\ 2f_D N_R \frac{1}{\xi}, & \xi > 1 \end{cases} \quad (44)$$

$D$  can be obtained by the clamping theorem. Observing (44), we know that when  $\xi = 1$ , the maximum normalized Doppler order is reached, and the maximum value is  $2f_D N_R$ .

### C. Coding Gain Loss in MRC-like Detection

In this section, the coding gain loss caused by imperfect CSI in MRC-like detection is derived, and the corresponding energy allocation scheme of minimum coding gain loss is obtained. As can be seen from [6], the coding gain in logarithmic form is:

$$\log C = - \lim_{\substack{\gamma_0 \rightarrow \infty \\ N \rightarrow \infty}} \left( \frac{\log(\bar{P}_e)}{N T_P D} + \log \gamma_0 \right) \quad (45)$$

Let  $\xi = 1$ , combine with (39), (40) and simplify to obtain the lower and upper bounds under perfect CSI:

$$\log C_L = \log 2C_M + \log \left( \frac{Kb}{(K+b)(N_T+b)} \right) + 1 - \log 2\delta \quad (46)$$

$$\log C_U = \log C_L - \frac{1}{2f_D T_P \pi v} \int_0^{\pi v} 2 \log(\sin \theta) d\theta \quad (47)$$

In the case of perfect CSI, no channel estimation is required,  $\gamma_0 = \gamma_C$ ,

$$(\mathbf{D})_{n,n} = \left( N_T - 1 + \Lambda_{PP}^{-1} (2\pi \frac{n-1}{N}) \right)^{-1}$$

corresponding,

$$\lim_{N \rightarrow \infty} \frac{\log(\Psi'_{t,k}(\gamma_0))}{N} = \frac{\delta}{\pi} \log(2c\gamma_C) - \frac{\delta \log 2\delta - \delta}{\pi} \quad (48)$$

The upper and lower bounds under perfect CSI:

$$\log C'_L = \log(2C_M) + 1 - \log 2\delta \quad (49)$$

$$\log C'_U = \log C'_L - \frac{1}{2f_D T_P \pi v} \int_0^{\pi v} 2 \log(\sin \theta) d\theta \quad (50)$$

According to the definition of [6],

$$\begin{aligned} \Upsilon_{\text{Loss}}(\text{dB}) &= 10 \log_{10} C'_U - 10 \log_{10} C_U \\ &= 10 \log_{10} C_L - 10 \log_{10} C_L \\ &= 10 \log_{10} \left[ \frac{(K+b)(N_T+b)}{Kb} \right] \end{aligned} \quad (51)$$

From the binary mean inequality, the minimum value of (51) is achieved when  $b = \sqrt{N_T K}$  and the minimum value is  $20 \log_{10} \left( 1 + \sqrt{N_T / K} \right)$  dB. Combining the above results, the maximum normalized Doppler diversity order is determined by the maximum Doppler spread  $f_D$  and the number of receiving antennas  $N_R$ . The minimum coding gain loss is determined by the number of transmitting antennas  $N_T$  and the number of data symbols in a block  $K$ .

## V. NUMERICAL RESULTS

In this section, we verify the correctness of the proposed theory by numerical results, and analyze the influence of various parameters on the spectral efficiency of MIMO systems using Doppler diversity under imperfect CSI. Consider a MIMO system operating at 1.9 GHz. The symbol transmission rate is  $10^5$  sym/s. Unless otherwise stated,  $N_T = 4$ ,  $N_R = 8$ ,  $K = 16$ ,  $N = 15$ , the modulation type is 4PSK. Pilot and data SNR  $\gamma_C$  and  $\gamma_P$  are both 10dB.

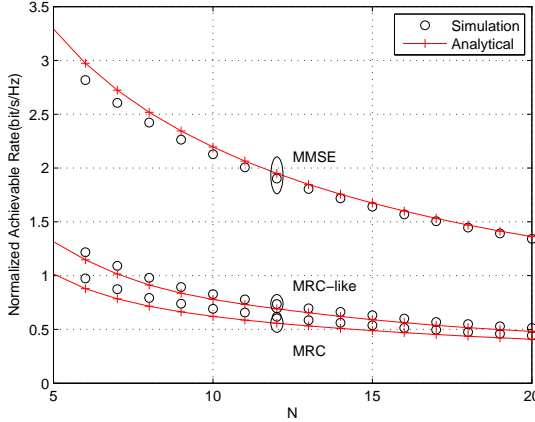


Fig. 2. Normalized achievable sum-rates of different Receivers as functions of  $N$  at  $k=1$

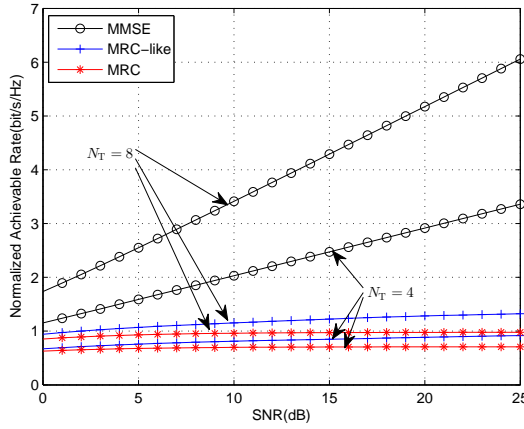


Fig. 3. Normalized achievable sum-rates as functions of SNR under low speed at  $k=1$

Without loss of generality, we first draw the ergodic normalized achievable sum-rates and corresponding analytical asymptotic results of the three receiving methods under different repetition times  $N$  when  $k$  takes 1. The speed is set to 113.6 km/h, corresponding to the 200 Hz Doppler spread. The number of receiving antennas  $N_R=4$ . The simulation results are obtained by Monte Carlo method, and the corresponding results of each point in the graph are obtained by averaging over 10,000 trials. It can be seen from the figure that the MMSE receiver has better performance. As  $N$  increases, the normalized sum-rate of each receiver decreases. This means that the spectral efficiency of the system will decrease with the increase of the number of repetitions. By comparing the achievable sum-rates of the three receivers, it is found that the performance gap narrows gradually with the increase of time of repetition. On the other hand, it can also be seen that the ergodic results are in good agreement with the corresponding analytical asymptotic results, which proves the correctness of the derivations in this paper.

Fig.3 reflects the change of normalized sum-rates with SNR at lower mobile speed. Since the correctness of the analytical

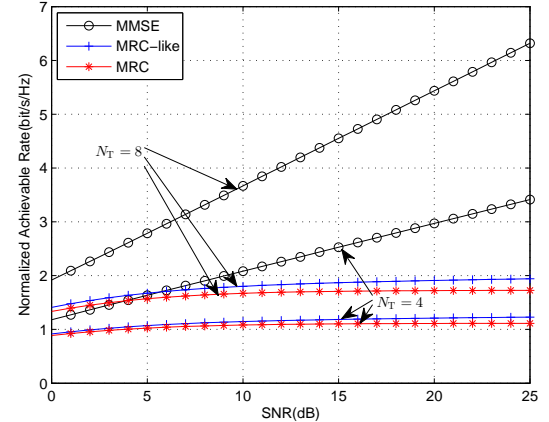


Fig. 4. Normalized achievable sum-rates as functions of SNR under high speed at  $k=1$

results has been verified above, the analytical results are directly used here for calculation. The Doppler spread of the system is 200 Hz. The analytical results of three receivers with different SNR when  $N_T=4$  and  $N_T=8$  are calculated respectively. The number of receiving antennas  $N_R=8$  ensures the normal operation of the space multiplexing receiver. As can be seen from the figure, as each transmitting antenna transmits different code words, the system can obtain greater spatial multiplexing gain and higher achievable sum-rate when the number of transmitting antennas increases. By comparing the three receivers, we can also find that the normalized sum-rate of MMSE receiver at  $k=1$  increases with the increase of pilot and data symbol SNR under any given  $N_T$ , while the achievable rate of MRC receiver hardly changes when the SNR increases to a certain extent, which is due to the MRC receiver poor ability to suppress interference, and the interference will limit the performance of the system when  $N_T$  is limited and fixed. Considering the interference from other antennas, the sum-rate of MRC-like receiver can keep increasing with the increase of SNR, and the performance is between the first two receivers.

In order to study the system at high speed, we keep the other parameters unchanged in Fig.4, and increase the speed to 568.4 km/h to obtain the achievable sum-rates of three receivers in high mobility scenarios. At this speed, the Doppler spread will reach 1 kHz. As can be seen from the figure, since the pilot interval still satisfies the requirement of  $(N_T + K) T \leq 0.5/f_D$ , the system can still work normally. Similar to the low speed, the achievable rates of the three receivers increase with the number of transmit antennas. Similar to the low speed, the achievable sum-rates of the three receivers increase with the number of transmit antennas, the performance of MMSE receiver steadily increases with the increase of the SNR, the performance of the MRC receiver is limited by the interference, and the performance of MRC-like receiver is between the two. By comparing Fig.3 and Fig.4, we find that MIMO systems with repetitive coding can achieve a slightly higher rate in high mobility scenarios. This is because at the same sampling rate, the correlation of

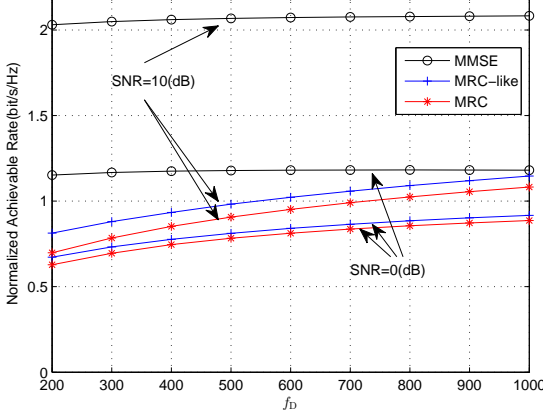


Fig. 5. Normalized achievable sum-rates as functions of  $f_D$  at  $k=1$

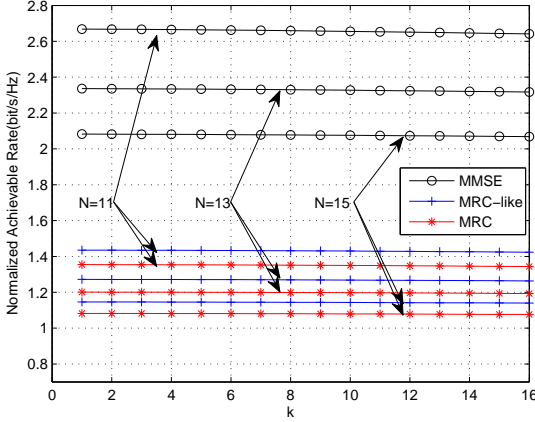


Fig. 6. Normalized achievable sum-rates as functions of  $k$

channel information corresponding to the repetitive coded data is weakened. Compared to MMSE receiver, MRC receiver and MRC-like receiver gain more.

In order to have a more intuitive understanding of the influence of different  $f_D$  on the normalized achievable sum-rate, we calculated the normalized achievable sum-rates under different  $f_D$  in Fig.5. The range of  $f_D$  is 200 Hz to 1000 Hz, i.e. the speed is 113.6 km/h to 568.4 km/h. The figure shows that in the system described in this paper, the increase of  $f_D$  can significantly improve the performance of MRC receiver and MRC-like receiver, but has little effect on MMSE receiver.

In Fig.6, we calculate the analytical results of three receivers corresponding to different values of  $k$  and  $N$  in the high mobility scene with 568.4 km/h, namely 1000Hz Doppler spread. From the figure, we can see that under the simulation environment we set up, when other conditions are fixed, the normalized achievable sum-rates of different  $k$  are basically the same. This means that when other conditions are the same, the performance of different locations in repetitive coding is basically the same.

In Fig.7, we calculate the normalized achievable sum-rates of three receivers at 568.4 km/h under large  $N_T$ . In order to

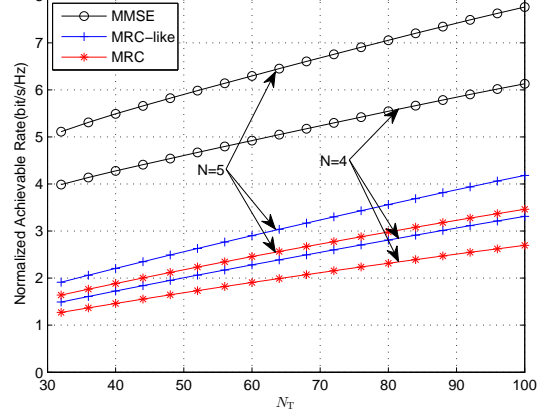


Fig. 7. Normalized achievable sum-rates as functions of  $N_T$  at high speed and large  $N_T$

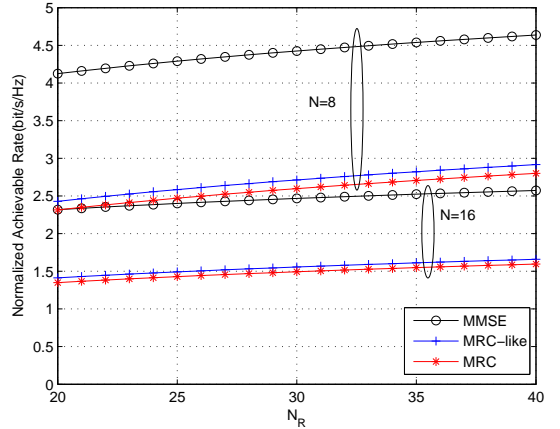


Fig. 8. Normalized achievable sum-rates as functions of  $N_R$

ensure the normal operation of the system, we set the symbol transmission rate to  $3 \times 10^5$  sym/s and let  $NN_R = 100$ . As can be seen from the figure, when  $N_T$  is large, the trend of influence of  $N_T$  on system performance is consistent with Fig.3 and Fig.4. This means that under the environment parameters we set, more spatial degree of freedom gains from transmitting antennas will help to improve the overall performance of the system.

Fig.8 studies the normalized achievable sum-rates of different receivers with  $N_R$  at high speed. The value of  $N$  is 8 or 16, which means that the maximum value of  $NN_R$  is 640. In this case, with the increase of the number of receiving antennas, the system obtains more spatial degrees of freedom, and the system performance of the three receivers is improved. When other conditions are fixed, the performance gap between receivers is basically fixed.

In Fig.9, the normalized achievable sum-rates of three receivers at high speed under large  $N$  have been studied as the value of  $N$  changes, set  $N_R$  to 20. The figure shows that the performance gap of the three receivers tends to disappear in the process of increasing  $N$ , which means that the normalized achievable sum-rates of the three receivers will converge when

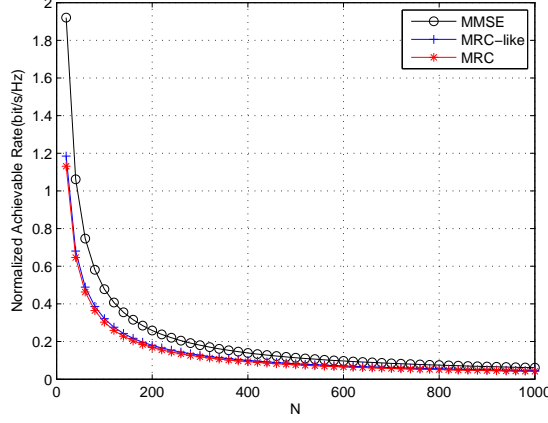


Fig. 9. Normalized achievable sum-rates as functions of  $N$  at high speed and large  $N$

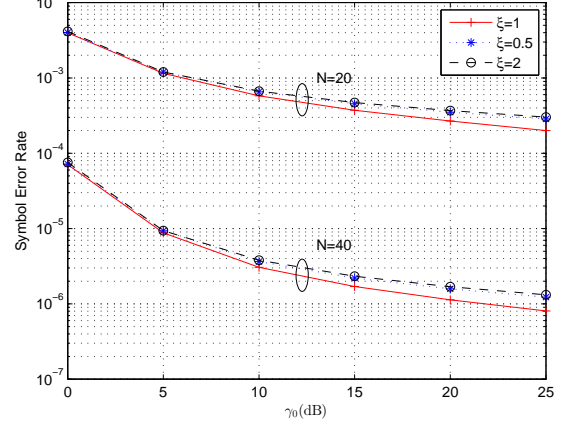


Fig. 11. SERs of the MRC-like receiver as functions of  $\gamma_0$

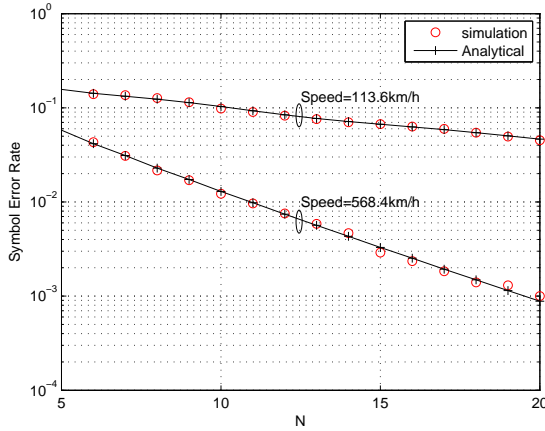


Fig. 10. SERs of the MRC-like receiver as functions of  $N$

$N$  tends to infinity.

The error rate of the MRC-like receiver is calculated in Fig.10. The analytical result is obtained by (37), both  $t$  and  $k$  are 1,  $N_R=4$ ,  $N=20$ . It can be seen that the simulation results and the analytical results match each other, which proves the correctness of the proposed theory. In addition, it can be seen that as  $N$  increases, the SER decreases steadily, and the speed of decreasing at a high speed is faster, which is because the Doppler order that can be obtained at a high speed is higher.

Fig.11 reflects the case where the SER changes with  $\gamma_0$  in the finite case of  $N$ . By definition,  $\gamma_0=(1/K)\gamma_p+\gamma_c$ , choose  $N_R=4$ , the speed is 568.4km/h and  $b=\sqrt{N_T K}$ . When  $N$  is finite, the decreasing speed of SER of MRC-like method decreases with the increase of  $\gamma_0$  while increases with the increase of  $N$ . The simulation results under different  $\xi$  values show that better performance can be achieved under  $\xi=1$ , which is consistent with the conclusion achieved when  $N$  tends to infinity.

Fig.12 simulates the change of SER with  $b$  in the case of limited  $N$ ,  $N_R=4$ , speed 568.4km/h and  $\xi=1$ . Since the perfect CSI does not need to consider pilot and data energy allocation, the SER performance is fixed, so the optimal performance

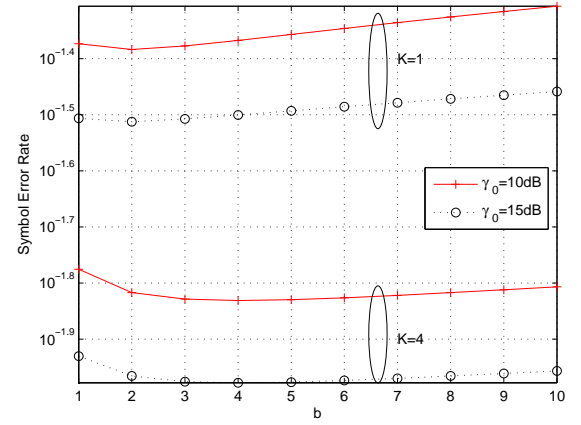


Fig. 12. SERs of the MRC-like receiver as functions of  $b$

under imperfect CSI corresponds to the minimum performance loss. The graph shows that when  $N$  is finite, the system has the best performance when  $b=\sqrt{N_T K}$ , which is consistent with the conclusion when  $N$  tends to infinity.

## VI. CONCLUSIONS

In this paper, the performance of MIMO system using repetitive coding to achieve Doppler diversity in high mobility scenarios is analyzed. Based on MMSE channel estimation, the equivalent channel model is derived and the asymptotic expressions of output SINR for MRC, MMSE and MRC-like receivers are obtained. The SER of MRC-like receiver is also derived, and the maximum normalized Doppler diversity order and corresponding conditions are obtained when  $N$  and  $\gamma_0$  tend to be infinite, i.e. the pilot energy changes linearly with the symbol energy of data, and the corresponding conditions when the minimum coding gain loss is obtained, i.e. the linear parameter  $b=\sqrt{N_T K}$ , the results obtained by simulation in the non-limiting state are consistent with the conclusions obtained of theoretical analysis in limit state.

The effects of different system configurations and channel parameters on system performance are also studied. The

simulation results show that in a high-speed MIMO system using repetitive coding, when the repetition times are limited, the achievable sum-rates of MMSE receiver are higher than those of the other two receivers in all cases. In high mobility scenarios, the increase of speed can increase the sum-rate of the system. For systems using MMSE receiver, the increase is almost negligible. For systems using MRC and MRC-like receiver, the increase of speed is more obvious. The gap between MMSE receivers and the other two receivers decreases, but the overall gap remains. For any receiver, the sum-rate obtained at different positions in repetitive coding is basically the same. Increasing the number of repetitions will reduce the normalized achievable sum-rate. Increasing the number of transmitting and receiving antennas will increase the degree of spatial freedom, thus the normalized achievable sum-rate will be increased.

## REFERENCES

- [1] J. Wu and P. Fan, "A survey on high mobility wireless communications: Challenges, opportunities and solutions," *IEEE Access*, vol. 4, pp. 450–476, 2017.
- [2] J. Zhao, Y. Liu, G. Yi, C. Wang, and L. Fan, "A dual-link soft handover scheme for C/U plane split network in high-speed railway," *IEEE Access*, vol. PP, no. 99, pp. 1–1, 2018.
- [3] A. M. Sayeed and B. Aazhang, "Joint multipath-Doppler diversity in mobile wireless communications," *IEEE Transactions on Communications*, vol. 47, no. 1, pp. 123–132, 1999.
- [4] M. Baissas and A. M. Sayeed, "Channel estimation errors versus Doppler diversity in fast fading channels," in *Conference on Signals, Systems & Computers*, 2000.
- [5] W. Zhou, J. Wu, and P. Fan, "High mobility wireless communications with Doppler diversity: Fundamental performance limits," *IEEE Transactions on Wireless Communications*, vol. 14, no. 12, pp. 6981–6992, 2015.
- [6] M. A. Mahamadu, J. Wu, M. Zheng, W. Zhou, Y. Tang, and P. Fan, "Fundamental tradeoff between Doppler diversity and channel estimation errors in SIMO high mobility communication systems," *IEEE Access*, vol. PP, no. 99, pp. 1–1, 2018.
- [7] T. L. Marzetta, "Noncooperative cellular wireless with unlimited numbers of base station antennas," *IEEE Transactions on Wireless Communications*, vol. 9, no. 11, pp. 3590–3600, 2010.
- [8] J. Zhao, S. Ni, Y. Gong, and Q. Zhang, "Pilot contamination reduction in TDD-based massive MIMO systems," *IET Communications*, vol. 13, no. 10, pp. 1425–1432, 2019.
- [9] D. Wang, Y. Zhang, H. Wei, X. You, X. Gao, and J. Wang, "An overview of transmission theory and techniques of large-scale antenna systems for 5G wireless communications," *Science China Information Sciences*, vol. 59, no. 8, p. 081301, 2016.
- [10] Y. Li, X. Gao, X. G. Xia, M. Ni, and P. Yan, "Pilot reuse for massive MIMO transmission over spatially correlated Rayleigh fading channels," *IEEE Transactions on Wireless Communications*, vol. 14, no. 6, pp. 3352–3366, 2015.
- [11] Y. Li, X. Gao, A. L. Swindlehurst, and Z. Wen, "Channel acquisition for massive MIMO-OFDM with adjustable phase shift pilots," *IEEE Transactions on Signal Processing*, vol. 64, no. 6, pp. 1461–1476, 2016.
- [12] L. You, X. Gao, G. Y. Li, X. G. Xia, and N. Ma, "BDMA for millimeter-wave/Terahertz massive MIMO transmission with per-beam synchronization," *IEEE Journal on Selected Areas in Communications*, vol. 35, no. 7, pp. 1550–1563, 2017.
- [13] S. Ning and J. Wu, "Maximizing spectral efficiency for high mobility systems with imperfect channel state information," *IEEE Transactions on Wireless Communications*, vol. 13, no. 3, pp. 1462–1470, 2014.
- [14] J. Hua, L. Meng, X. Xu, D. Wang, and X. You, "Novel scheme for joint estimation of SNR, Doppler, and carrier frequency offset in double-selective wireless channels," *IEEE Transactions on Vehicular Technology*, vol. 58, no. 3, pp. 1204–1217, 2009.
- [15] M. Wang and D. Wang, "Sum-rate of multi-user MIMO systems with multi-cell pilot contamination in correlated Rayleigh fading channel," *Entropy*, vol. 21, no. 6, 2019. [Online]. Available: <https://www.mdpi.com/1099-4300/21/6/573>
- [16] J. Cao, D. Wang, L. I. Jiamin, Q. Sun, and H. U. Ying, "Uplink spectral efficiency analysis of multi-cell multi-user massive MIMO over correlated Ricean channel," *Science China(Information Sciences)*, vol. v.61, no. 8, pp. 195–208, 2018.
- [17] R. Couillet and M. Debbah, "Random matrix methods for wireless communications," *IEEE Expert*, vol. 5, no. 3, pp. 16–23, 2012.
- [18] J. Cao, D. Wang, X. Duan, J. Li, and X. You, "Uplink symbol error rate analysis of multicell multiuser-multiple-input multiple-output systems with minimum mean square error receiver under pilot contamination," *IET Communications*, vol. 10, no. 9, pp. 1121–1129, 2016.
- [19] Gazzah, Houceme, Regalia, A. Phillip, Delmas, and Jean-Pierre, "Asymptotic eigenvalue distribution of block Toeplitz matrices and application to blind SIMO channel identification," *IEEE Transactions on Information Theory It*, vol. 47, no. 3, pp. 1243–1251, 2001.



**Xiaoyun Hou** received the B.S. degree and the M.S. degree from Nanjing University of Posts and Telecommunications in 1999 and 2002, and the Ph.D. degree from Shanghai Jiaotong University in 2005. She joined Nanjing University of Posts and Telecommunications, China, in 2005, where she has been an Associate Professor since 2009. She was a visiting scholar at University of California, Davis, CA from 2012 to 2013. Her current research interests include signal processing techniques in high mobility MIMO communications.



**Jie Ling** received the B.S. degree from Nanjing University of Posts and Telecommunications in 2017, where currently he is working for the M.S. degree. His current research interests include signal processing techniques in high mobility MIMO communications.



**Dongming Wang** received the B.S. degree from Chongqing University of Posts and Telecommunications in 1999, the M.S. degree from Nanjing University of Posts and Telecommunications in 2002, and the Ph. D. degree from Southeast University in 2006. He joined the National Mobile Communications Research Laboratory at Southeast University, China, in 2006, where he is a Professor now. He serves as an associate editor for the SCIENCE CHINA Information Sciences. His current research interests include channel estimation, distributed antenna systems, and large-scale MIMO systems.